Activation properties of Kv4.3 channels: time, voltage and $[K^+]_o$ dependence

Shimin Wang[1,2], Vladimir E. Bondarenko[1], Yujie Qu[1], Michael J. Morales[1], Randall L. Rasmusson[1] and Harold C. Strauss[1]

[1] *Department of Physiology and Biophysics, University at Buffalo, SUNY, School of Medicine and Biomedical Sciences, Buffalo, NY, USA and* [2] *Department of Cardiology, Renmin Hospital of Wuhan University, 238 Jiefang Road, Wuhan, Hubei, China*

Rapidly inactivating, voltage-dependent K^+ currents play important roles in both neurones and cardiac myocytes. Kv4 channels form the basis of these currents in many neurones and cardiac myocytes and their mechanism of inactivation appears to differ significantly from that reported for *Shaker* and Kv1.4 channels. In most channel gating models, inactivation is coupled to the kinetics of activation. Hence, there is a need for a rigorous model based on comprehensive experimental data on Kv4.3 channel activation. To develop a gating model of Kv4.3 channel activation, we studied the properties of Kv4.3 channels in *Xenopus* oocytes, without endogenous KChIP2 ancillary subunits, using the perforated cut-open oocyte voltage clamp and two-electrode voltage clamp techniques. We obtained high-frequency resolution measurements of the activation and deactivation properties of Kv4.3 channels. Activation was sigmoid and well described by a fourth power exponential function. The voltage dependence of the activation time constants was best described by a biexponential function corresponding to at least two different equivalent charges for activation. Deactivation kinetics are voltage dependent and monoexponential. In contrast to other voltage-sensitive K^+ channels such as HERG and *Shaker*, we found that elevated extracellular $[K^+]$ modulated the activation process by slowing deactivation and stabilizing the open state. Using these data we developed a model with five closed states and voltage-dependent transitions between the first four closed states coupled to a voltage-insensitive transition between the final closed (partially activated) state and the open state. Our model closely simulates steady-state and kinetic activation and deactivation data.

(Received 23 November 2003; accepted after revision 2 March 2004; first published online 5 March 2004)
Corresponding author S. Wang: Department of Physiology and Biophysics, UB, SUNY, School of Medicine and Biomedical Sciences, 124 Sherman Hall, 3435 Main Street, Buffalo, NY 14214, USA. Email: swang2@acsu.buffalo.edu

Rapidly inactivating, voltage-dependent K^+ channels play important roles in both neurones and cardiac myocytes. In pre- and postsynaptic neurones, rapid (A-type) inactivating K^+ currents can strongly modulate excitability, thereby influencing events such as interspike interval (Hille, 2001). In the heart, the rapidly inactivating voltage-dependent K^+ current, I_{to}, contributes to the action potential plateau and, as a result, to the magnitude of Ca^{2+} influx during the plateau. In addition, these K^+ currents also determine the duration of repolarization and the propensity to cardiac arrhythmias (Campbell *et al.* 1995; Brahmajothi *et al.* 1999; Nerbonne, 2000; Strauss *et al.* 2001; Antzelevitch & Shimizu, 2002). It is currently accepted that Kv4 channels form the basis of these currents in many neurones and cardiac myocytes (Jerng & Covarrubias, 1997; Brahmajothi *et al.* 1999; Nerbonne *et al.* 2001).

The cardiac I_{to} is formed by the association of Kv4.2 and Kv4.3 α subunits with KChIP2 ancillary subunits (An *et al.* 2000; Patel *et al.* 2002*a*,*b*; Rosati *et al.* 2003). Recent studies have demonstrated that the Kv4.2 and Kv4.3 channel α subunits associate with KChIP ancillary subunits, and that both are colocalized in the ventricular myocardium (Patel *et al.* 2002*a*,*b*; Rosati *et al.* 2003). Although this family of ancillary subunits has been demonstrated to increase the expression of K^+ channels, they also have been shown to modify the gating of the Kv4 channels. However, the underlying mechanism(s) is unresolved.

Kv4 channels have recently attracted great interest because their mechanism of inactivation appears to differ

© The Physiological Society 2004 DOI: 10.1113/jphysiol.2003.058578

significantly from that reported for *Shaker* and Kv1.4 channels. In *Shaker* and Kv1.4 channels, inactivation is governed by N- and C-type inactivation attributed to a ball and chain mechanism occluding the inner vestibule (N-type) and pore closure (C-type) (Hoshi *et al.* 1991; Liu *et al.* 1996; Rasmusson *et al.* 1998; Jiang *et al.* 2003*a*; Gebauer *et al.* 2004). In contrast, Jerng & Covarrubias (1997) and Jerng *et al.* (1999) showed that inactivation in Kv4.1 channels occurs from both a partially activated closed and an open state. In most ion channels, inactivation is coupled to activation (Bezanilla & Armstrong, 1977; Papazian *et al.* 1991; Hille, 2001). As a result, models of inactivation are critically dependent on the kinetics and steady-state activation and deactivation properties. Currently, activation data on the Kv4.3 α subunit expressed in the absence of an ancillary subunit is incomplete, either because the appropriate kinetic data were not obtained or because the Kv4.3 α subunit was expressed in cells containing an endogenous KChIP2 ancillary subunit (Jerng *et al.* 1999; Bähring *et al.* 2001; Beck *et al.* 2002; Patel *et al.* 2002*a*). In all cases, models of Kv4.x activation have not been developed from a rigorous comparison of the experimental steady-state and kinetic activation and deactivation data.

While significant progress has been made in our understanding of the biophysical basis of gating of Kv4 channels, especially Kv4.1 channel inactivation gating, further study of Kv4.3 channel activation gating kinetics was warranted for four important reasons. First, Kv4.3 channels form the basis of the cardiac I_{to} in several animal species and the human heart (Näbauer *et al.* 1993; Brahmajothi *et al.* 1999; Nerbonne *et al.* 2001). Second, Kv4.1 and Kv4.3 channels display significant functional differences (Jerng & Covarrubias, 1997; Jerng *et al.* 1999; Beck & Covarrubias, 2001). Third, the model developed by Bähring *et al.* (2001) was based on a study of heterologously expressed Kv4.2 channels in HEK293 cells, which contain an endogenous KChIP protein (Patel *et al.* 2002*a*). Finally and most importantly, the development of a model of activation that is based on accurate measurements is a foundation for any model of inactivation.

Therefore, in this paper, we set out to systematically study the properties of Kv4.3 channels in a heterologous expression system that did not express endogenous KChIP2 ancillary subunits (Patel *et al.* 2002*a*). A comprehensive analysis of activation of Kv4.3 currents expressed in *Xenopus* oocytes was implemented using the cut-open oocyte voltage clamp technique. We obtained high-frequency resolution measurements of the activation properties of Kv4.3 channels and developed a discrete state Markov model that closely describes the experimental data. The voltage dependence of the activation time constants was best described by a biexponential function corresponding to at least two different equivalent charges for activation. Our analysis suggests that the equivalent charge movement during activation can vary as a function of voltage. Finally, in contrast to other voltage-sensitive K^+ channels (HERG, *Shaker*), we found that markedly elevated extracellular K^+ concentrations modulated the activation process by slowing deactivation and stabilizing the open state.

Methods

cRNA preparation and channel expressions

Wild type (WT) cDNA of Kv4.3 channels (short form), a gift of Dr David McKinnon (Stony Brook, SUNY) was utilized in these studies. The construct has been previously described (Wang *et al.* 2002).

Mature female *Xenopus laevis* (Xenopus One, Ann Arbor, MI, USA) were anaesthetized by immersion in tricaine solution (1.5 g l^{-1}). Ovarian lobes were removed through a small incision in the abdominal wall. The follicular layer was removed enzymatically by placing the lobes in a collagenase-containing, Ca^{2+}-free OR2 solution (mM): 82.5 NaCl, 2 KCl, 1 $MgCl_2$, 5 Hepes, pH 7.4; 1–2 mg ml^{-1} collegenase (Type I, Sigma, St Louis, MO, USA). After removal of the ovarian lobe, the incisions were sutured closed and the frogs were then allowed to recover in a small water-filled container as previously described (Comer *et al.* 1994). Typically, lobes were obtained three times from a single frog. When individual frogs no longer yielded acceptable oocytes, they were anaesthetized and killed by an overdose of tricaine (20 g l^{-1}).

The oocytes were gently shaken for about 2 h and collagenase activity was then halted by bovine albumin as previously described (Comer *et al.* 1994). Defolliculated oocytes (stage V–VI) were then injected with transcribed cRNA (up to 50 nl) using a 'Nanoject' microinjection system (Drummond Scientific Co., Broomall, PA, USA) and incubated at 18°C for 24–72 h in an antibiotic-containing Barth's solution (mM): 88 NaCl, 1 KCl, 2.4 $NaHCO_3$, 0.82 $MgSO_4$, 0.33 $Ca(NO_3)_2$, 0.41 $CaCl_2$, 10 Hepes (pH: 7.4), 2% (v/v of 100 × stock) antibiotic–antimycotic (Invitrogen).

Electrophysiological techniques

Experiments were performed using a cut-open oocyte clamp amplifier (CA-1b, Dagan Corp., Minneapolis, MN, USA) (Taglialatela *et al.* 1992) as previously described (Comer *et al.* 1994). Microelectrodes were fabricated from 1.5 mm o.d. borosillicate glass tubing

© The Physiological Society 2004

(TW150F-4, WPI) using a two-stage puller (L/M-3 P-A, Adams & List Associates, Ltd, Great Neck, NY, USA) filled with 3 M KCl with resistances of 0.6–1.5 MΩ. During recording, oocytes were continuously superfused externally (upper pool) with control ND 96 solution (mM): 96 NaCl, 2 KCl, 1 $MgCl_2$, 1.8 $CaCl_2$, 10 Hepes, pH 7.4, adjusted with NaOH or ND 98 solution (mM): 98 KCl, 1 $MgCl_2$, 1.8 $CaCl_2$, 10 Hepes, pH 7.4 adjusted with NaOH. The composition of the upper and middle (guard) pool solutions were identical. Intracellular (lower pool) solution contained (mM): 98 KCl, 1.8 $MgCl_2$, 1 EGTA and 5 Hepes-NaOH, pH 7.4. Currents were recorded at room temperature (21–23°C) and were sampled at 250 kHz. The time resolution of decay was determined by the time constants of capacitance transients that were in the range of 50–125 μs. Currents from the cut-open oocyte clamp technique were leakage and capacitance subtracted using a *P*/4 pulse protocol, unless otherwise noted. Cut-open oocyte clamp data were filtered at 10 kHz.

Experiments were also performed on oocytes using a two-microelectrode bath clamp amplifier (OC-750A, Warner Instruments Corp., Hamden, CT, USA) as has been described in detail elsewhere (Comer *et al.* 1994). Microelectrodes were fabricated from 1.5 mm o.d. borosilicate glass tubing (TW150F-4, WPI) using a two-stage puller (L/M-3 P-A, Adams & List Associates) to produce electrodes with resistances of 0.6–1.5 MΩ when filled with 3 M KCl. During recording, oocytes were continuously perfused with control solution (mM: 96 NaCl, 2 KCl, 1 $MgCl_2$, 1.8 $CaCl_2$ and 10 Hepes, adjusted to pH 7.4 with NaOH) or 98K solution (mM: 98 KCl, 1 $MgCl_2$, 1.8 $CaCl_2$ and 10 Hepes, adjusted to pH 7.4 with NaOH). Solutions with 5, 10 and 50 mM KCl contained 93, 88 and 48 mM NaCl, respectively. Currents were recorded at room temperature (21–23°C) and were sampled at 20 kHz. The two-electrode voltage clamp data were filtered at 10 kHz.

Data analysis

Data were recorded on a computer and were digitized and analysed directly using pCLAMP 9 and Clampfit 9 software (Axon Instruments, Inc.). The pulse protocols and the equations that best fit the data are presented in the corresponding figure legends. Data are shown as means ± S.E.M. Confidence levels were calculated using Student's paired *t* test. A fourth power Boltzmann function ($f(V) = 1/\{1 + \exp[-(V - V_{½})/k]\}^4$) was used to fit the data to calculate the steady-state activation relationship.

Gating model and simulation

For model development we used Fortran 90 and ran the program on DEC Alpha workstation. The Markov model was implemented as a set of evolution differential equations for five closed states, C_0–C_4, and one open state, O. One inactivated state, I, was added to simulate effect of inactivation on determination of the activation time constant τ_{act}. Numerical solution of differential equations was performed by fourth-order Runge-Kutta method. We assumed that initially, at a resting potential of −90 mV, all channels were in the state C_0, $C_0 = 1.0$, and all other states were empty.

Results

Activation

Prior studies that evaluated the kinetics of activation of Kv4.3 channels have been limited by the use of the two-electrode voltage clamp technique in the study of transfected oocytes or by the inadvertent use of a heterologous expression system containing endogenous KChIP2 subunits. With the standard two-electrode voltage clamp technique, the duration of the capacitive transient (~2 ms) could obscure the initial part of the relatively fast activation process of channels such as Kv4.3 (Taglialatela *et al.* 1992). Therefore, we set out to measure the kinetics of activation of Kv4.3 in transfected oocytes obtained from *Xenopus laevis* using the cut-open oocyte voltage clamp technique. As $[K^+]_o$ has been shown to modify the gating properties of this and other K^+ channels (Rasmusson *et al.* 1995, 1998; Wang *et al.* 1997; Eghbali *et al.* 2002), both the kinetics and steady-state activation relationships were measured at several $[K^+]_o$.

Typical responses of Kv4.3 channels to a series of test depolarizations illustrate the rapid activation and inactivation of the channel measured at 2 mM $[K^+]_o$ (Fig. 1*A*). As the study of the voltage dependence of activation can be compromised by fast inactivation, we set out to measure the activation properties using two series of depolarizing pulses, 10 and 1000 ms (Figs 1 and 2*A*, *B*). Ten-millisecond pulses were used to minimize inactivation. Activation data shown in Fig. 2*A* and *B* were obtained following capacitance subtraction and demonstrated a sigmoid delay and voltage dependence. The voltage dependence was manifest by an increase in both the rate of activation and the magnitude of the current. The sigmoidal activation time course was fitted with a Hodgkin–Huxley-like activation equation of the general form $C[1 - \exp(-t/\tau_{act})]^n$, where C is a constant and n was allowed to vary between 1 and 5. Optimal fits

© The Physiological Society 2004

were obtained at $n = 4$ and 5, but the difference was not significant and as a result a value of $n = 4$ was selected for subsequent analysis (Fig. 1*B*).

To examine the effects of elevated $[K^+]_o$ on activation, we initially compared activation data at 2 mM $[K^+]_o$ with those at 98 mM $[K^+]_o$ and demonstrated that the currents at 98 mM $[K^+]_o$ were smaller at all potentials than at 2 mM $[K^+]_o$ (Fig. 2*A* and *B*). These differences could be attributed to a reduced electrochemical gradient. Peak *I–V* relationship at 2 mM $[K^+]_o$ was linear at voltages positive to −10 mV and demonstrated a threshold for activation of −40 mV (Fig. 3*A*, unfilled circles). At 98 mM $[K^+]_o$ (Fig. 3*A*, filled circles), activation threshold was shifted to more negative potentials when compared to 2 mM $[K^+]_o$. The best fit of steady-state activation data at 2 mM $[K^+]_o$ (Fig. 3*B*, unfilled circles) using a fourth-power Boltzmann function, $f(V) = 1/\{1 + \exp[-(V - V_{½})/k]\}^4$, yielded a $V_{½}$ of − 29.4 mV and a k of 19.4 mV. This k-value corresponds to an equivalent charge of $1.31e_0$ per subunit. At 98 mM $[K^+]_o$ (Fig. 3*B*, filled circles), the same fitting function yielded a $V_{½}$ of −37.7 mV and a k of 18.2 mV, which corresponds to an equivalent charge of $1.40e_0$ per subunit. As the slope factor of macroscopic current will only provide a lower limit of the charge movement per subunit, the estimates of equivalent charge represent a minimal value (Schoppa *et al.* 1992; Aggarwal & MacKinnon, 1996; Seoh *et al.* 1996).

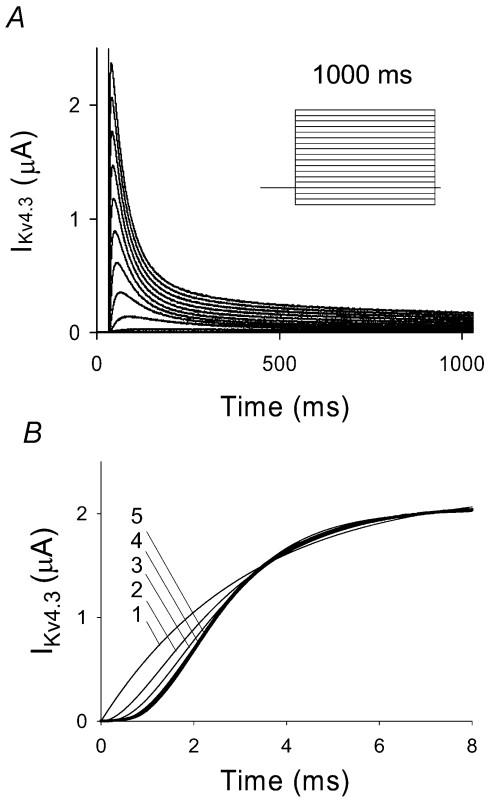

Figure 1. Experimental Kv4.3 current
A, experimental traces of Kv4.3 current recorded using a holding potential of −90 mV and a series of 1000 ms depolarizing pulses from −120 to +50 mV in 10 mV steps at an extracellular K^+ concentration of 2 mM using the cut-open oocyte voltage clamp technique. Inset, voltage clamp protocol, used for generation of $I_{Kv4.3}$ traces. *B*, comparison of the time course of experimental $I_{Kv4.3}$ at depolarization to +50 mV (10 ms pulse) and fitting by function $f_a(t) = C(1 - \exp[-t/\tau_{act}])^n$, where n is varied from 1 to 5. In the cases of $n = 4$ and $n = 5$, the function $f_a(t)$ gave the best fit to the experimental data.

The voltage dependence of activation time constants was measured using both 10 and 1000 ms pulses at 2 mM $[K^+]_o$ and is shown in Fig. 3*C*. Substantial differences in the voltage dependence of activation were observed. The relationship obtained from fitting the rising phase of current traces recorded with 1000 ms pulses was much steeper than with 10 ms pulses. Closer analysis revealed that activation kinetics (τ_{act}) determined with 10 and 1000 ms (unfilled triangles and circles, respectively) closely approximated each other between 0 and +50 mV. However, the steep voltage dependence seen with 1000 ms pulses between −40 and 0 mV was not observed with 10 ms pulses, reflecting truncation of slower activation processes. For example, 1000 and 10 ms pulses at −30 mV yield substantial differences in the value of τ_{act} ($\tau_{act} = 9.6$ ms and 4.3 ms, respectively). These substantial differences in the values of τ_{act} indicate that use of short duration pulses results in an underestimation of τ_{act} and precludes the use of a 10 ms pulse to characterize activation kinetics at these potentials. On the other hand the rising phase of the current during longer pulses, used to estimate τ_{act}, can be influenced by inactivation.

The next analysis of activation kinetics was performed using data obtained with 1000 ms pulses. At voltages positive to 0 mV the voltage dependence of τ_{act} was much more shallow than at more negative potentials. As a result, voltage dependence of activation could not be fitted adequately by a single exponential function (dashed line in Fig. 3*C*); however, the experimental values were well fitted by a biexponential function. At 98 mM $[K^+]_o$, the voltage dependence of activation kinetics between −40 and −10 mV was less steep than at 2 mM $[K^+]_o$ (Fig. 3*C*) and at voltages positive to 0 mV, the voltage dependence was even less apparent. Activation kinetics converged at positive potentials at the two different $[K^+]_o$. Using the values derived from fitting with the biexponential function, the equivalent charges were found to be $0.27e_0$ and $2.11e_0$ per subunit for 2 mM $[K^+]_o$ and $0.23e_0$ and $1.24e_0$ per subunit for 98 mM $[K^+]_o$. These data indicate that less charge movement was needed to activate the Kv4.3 channel at high

© The Physiological Society 2004

$[K^+]_o$, particularly at smaller depolarizing pulses near the threshold for activation.

Deactivation

Deactivating tail current kinetics (τ_{deact}) were measured and shown to be monoexponential and voltage dependent (Fig. 4*A* and *B* for 2 and 98 mM $[K^+]_o$, respectively). Current traces shown in Fig. 4 are capacitance subtracted. At 2 mM $[K^+]_o$ deactivation currents were both inward and outward in the potential range between −120 to −50 mV (Fig. 4*A*), but at 98 mM $[K^+]_o$ only inward deactivation tail currents were observed (Fig. 4*B*). Deactivation kinetics were voltage dependent at both 2 and 98 mM $[K^+]_o$ and slower at 98 mM $[K^+]_o$ throughout the voltage range evaluated (Fig. 5*A*). The equivalent charges were $0.48e_0$ per subunit for 2 mM $[K^+]_o$ and a smaller value of $0.33e_0$ per subunit was obtained at 98 mM $[K^+]_o$.

To examine the $[K^+]_o$ dependence of activation over a physiological and pathophysiological range, we measured steady-state activation and deactivation at different $[K^+]_o$ ranging between 2 and 50 mM, using the two-electrode voltage clamp technique. Peak tail current values following a 10 ms P1 pulse from −90 to +50 mV (10 mV steps) were used to determine the steady-state activation relationships. Deactivation time constants were measured from tail currents held at −45 mV (250 ms) following a 10 ms P1 pulse to +50 mV. Data shown in Table 1 indicate that there were no significant effects of $[K^+]_o$ on $V_{½}$, k and τ_{deact} in the concentration range between 2 and 10 mM $[K^+]_o$. When comparisons were made for these three variables between 10 and 50 mM $[K^+]_o$ significant differences were observed for all three parameters (Table 1). The slope factor decreased, the $V_{½}$ shifted to more negative values, and τ_{deact} increased at 50 mM $[K^+]_o$.

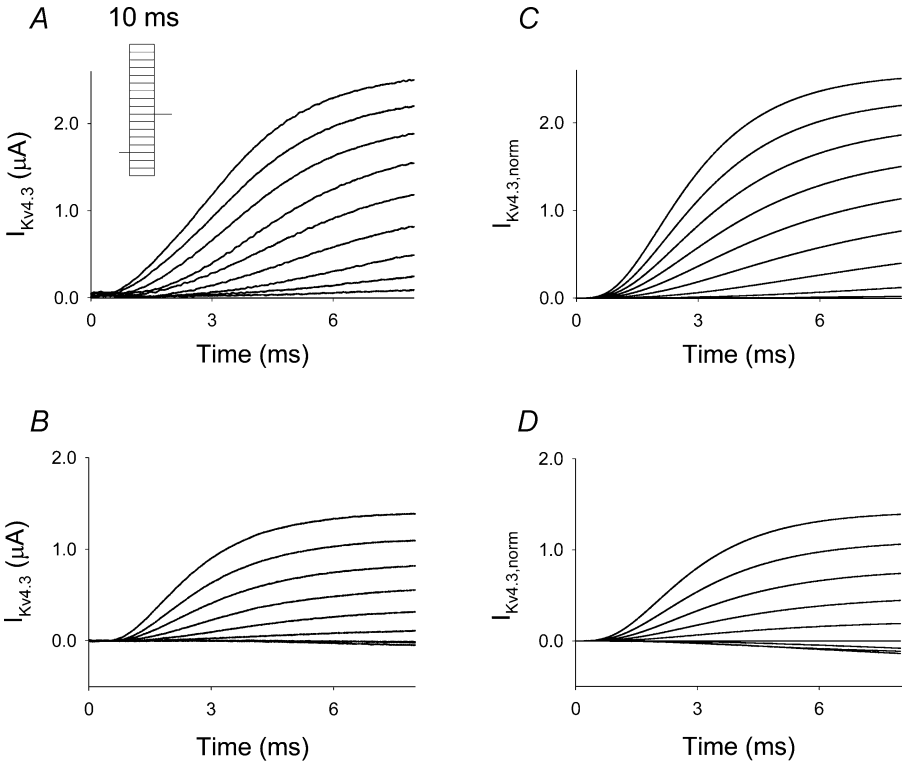

Figure 2. Series of experimental traces of activation of $I_{Kv4.3}$ obtained at different $[K^+]_o$, 2 mM (*A*) and 98 mM (*B*), and simulated traces of activation of $I_{Kv4.3}$ for different $[K^+]_o$, 2 mM (*C*) and 98 mM (*D*)
A series of 10 ms voltage steps were applied from a holding potential of −90 mV ranging between −120 and +50 mV in 10 mV steps using the cut-open voltage clamp technique. Capacitance transients were subtracted by fitting with exponential functions. Simulated traces were generated using the same experimental protocol as described above in *A* and *B* and are based on a discrete state Markov model. Depolarization pulses during simulations were applied at the end of a 20 ms holding potential at which time test depolarizations were initiated and designated as occurring at $t = 0$ ms. A 20 ms holding potential was used to allow the channel to reach equilibrium. Traces were normalized to the experimental value of $I_{Kv4.3}$ at the end of the depolarization pulse to +50 mV and at 2 and 98 mM $[K^+]_o$. Inset in *A*, voltage clamp protocol, used for generation of $I_{Kv4.3}$ traces.

© The Physiological Society 2004

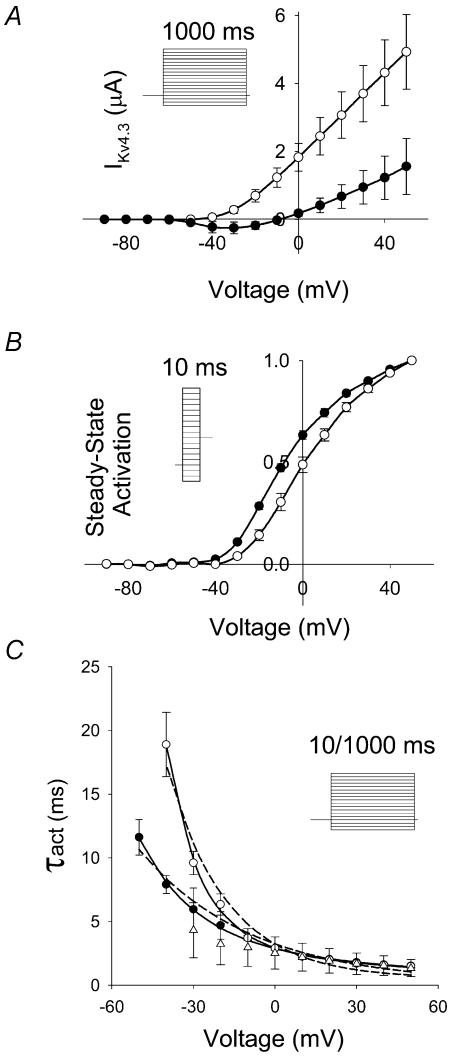

Figure 3. Effects of two different extracellular [K^+] on peak *I–V* relationship and activation properties
A, experimental *I–V* relationship for $I_{Kv4.3}$, 2 mM (○, $n = 5$) and 98 mM (●, $n = 4$). Data were obtained using 1000 ms voltage steps from a holding potential of −90 mV to variable voltages ranging between −120 and +50 mV in 10 mV steps (see inset in *A*). *B*, experimental steady-state activation functions were obtained for $I_{Kv4.3}$ using a two-pulse protocol. Ten-millisecond voltage pulses, P1, applied from a holding potential −90 mV ranged between −120 and +50 mV (10 mV increment), with P2 set at −40 mV and 500 ms duration (inset in *B*). Data recorded at $[K^+]_o$ 2 ($n = 3$) and 98 mM ($n = 5$), are represented by ○ and ●, respectively. *C*, the time constants of activation (τ_{act}) were determined by fitting the rising phase of $I_{Kv4.3}$ obtained during both 10 and 1000 ms depolarizing pulses (inset in *C*). Current traces were then fitted with the function $f_a(t) = C(1 - \exp(-t/\tau_{act}))^4$. The data obtained with a 1000 ms pulse are shown by ○ (2 mM $[K^+]_o$, $n = 5$) and ● (98 mM $[K^+]_o$, $n = 4$). Experimental data obtained at 2 mM $[K^+]_o$ using a 10 ms pulse ($n = 4$) are shown as △. Dashed and continuous lines show fits of $\tau_{act}(V)$ with single- and double-exponential functions, respectively. All data shown in this figure were obtained using the cut-open oocyte voltage clamp technique.

Discrete state Markov model and simulations of Kv4.3 channel activation

Experimental data were used to create a model for activation that contained five closed states and one open state. The rate constants of transitions between the closed states are voltage dependent, whereas the rate constant of transitions between the last closed state and the open state is voltage independent (Zagotta *et al.* 1994*b*). The model is shown in Scheme 1.

$$\begin{array}{ccccccc} & 4\alpha & 3\alpha & 2\alpha & \alpha & k_{co} & \\ C_0 & \rightleftharpoons & C_1 & \rightleftharpoons & C_2 \rightleftharpoons C_3 & \rightleftharpoons & C_4 \rightleftharpoons O \\ & \beta & 2\beta & 3\beta & 4\beta & k_{oc} & \end{array}$$

The forward and backward rate constants of activation for 2 mM $[K^+]_o$ are given by the following equations:

$$\alpha = f_\alpha(a_1 \exp(z_{\alpha 1} e_0 V F/RT) \exp((V + 10.0)/10.0) + a_2 \exp(z_{\alpha 2} e_0 V F/RT))$$

$$\beta = f_\beta(b_1 \exp(z_{\beta 1} e_0 V F/RT) \exp((V + 5.0)/10.0) + b_2 \exp(z_{\beta 2} e_0 V F/RT))$$

where factors

$$f_\alpha = 1/(1 + \exp((V + 10.0)/10.0))$$

$$f_\beta = 1/(1 + \exp((V + 5.0)/10.0))$$

Voltage-independent rate constants k_{co} and k_{oc} are equal to 6000 and 1500 s^{-1}, respectively. Equations for α and β were chosen so that they approach the exponential functions:

$$\alpha \propto \exp(z_{\alpha 1} e_0 V F/RT)$$

$$\beta \propto \exp(z_{\beta 1} e_0 V F/RT)$$

when $V \rightarrow +50$ mV and

$$\alpha \propto \exp(z_{\alpha 2} e_0 V F/RT)$$

$$\beta \propto \exp(z_{\beta 2} e_0 V F/RT)$$

when $V \rightarrow -120$ mV. In the case of high $[K^+]_o$ (98 mM), forward and backward rate constants of activation are described by equations

$$\alpha_K = f_{\alpha K}(a_{1K} \exp(z_{\alpha 1K} e_0 V F/RT) \exp((V + 25.0)/10.0) + a_{2K} \exp(z_{\alpha 2K} e_0 V F/RT))$$

$$\beta_K = f_{\beta K}(b_{1K} \exp(z_{\beta 1K} e_0 V F/RT) \exp((V + 20.0)/10.0) + b_{2K} \exp(z_{\beta 2K} e_0 V F/RT))$$

© The Physiological Society 2004

where

$$f_{\alpha K} = 1/(1 + \exp((V + 25.0)/10.0))$$

$$f_{\beta K} = 1/(1 + \exp((V + 20.0)/10.0))$$

The net current through the channel is given by

$$I_{Kv4.3} = G_{max} P_o (V - E_K)$$

where G_{max} is the maximum potassium conductance for that particular K^+ concentration, P_o is the open probability and E_K is given by the Nernst relationship below:

$$E_K = \frac{RT}{F} \ln \frac{[K^+]_o}{[K^+]_i}$$

The voltage-independent rate constant k_{co} is not changed at 98 mM $[K^+]_o$, but k_{oc} is decreased from 1500 to 1200 s^{-1}. The constants used in the equations are given in Table 2.

The decrease in k_{oc} at the higher $[K^+]_o$ reflects the slowed deactivation kinetics measured in our experiments. The slowed deactivation kinetics also led to a reduced value of β at high $[K^+]_o$ (β_K), which is smaller than the value of β at low $[K^+]_o$ (β). This decrease in β was also responsible for the shift in steady-state activation relationship shown in Fig. 3*B*.

Figure 2*C* and *D* shows simulated traces of Kv4.3 current obtained using a holding potential of −90 mV and a series of depolarizing steps from −80 to +50 mV (10 mV increments). The time course of the currents are similar to that observed in the experiment (compare to Fig. 2*A* and *B*). G_{max} was estimated from the measured current at the end of a 10 ms depolarizing pulse to +50 mV in 2 and 98 mM $[K^+]_o$. Simulated and experimental currents at 98 mM $[K^+]_o$ are correspondingly smaller at all voltages due to changes in driving force. The simulated time courses of Kv4.3 current deactivation for 2 and 98 mM $[K^+]_o$ are shown in Fig. 4*C* and *D*, respectively. In relatively low $[K^+]_o$, simulations and experiments produce both inward and outward tail currents, depending on the membrane

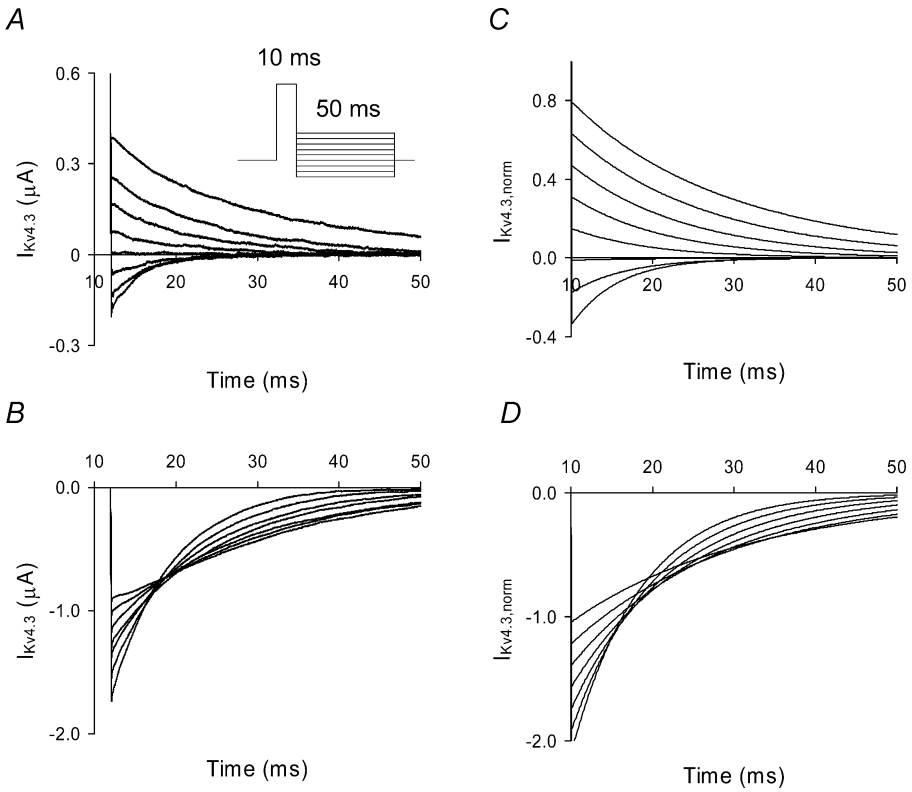

Figure 4. Effects of two different extracellular $[K^+]$ on deactivation of $I_{Kv4.3}$
Experimental records of deactivation at $[K^+]_o$ concentrations of 2 mM (*A*) and 98 mM (*B*) are shown. A two-pulse protocol was used. Holding potential was −90 mV and the P1 pulse was set to +50 mV for 10 ms and followed by a second pulse that ranged between −120 to −40 mV for 50 ms in steps of 10 mV (inset in *A*). Capacitance transients were subtracted. Simulated traces of deactivation of $I_{Kv4.3}$ for different $[K^+]_o$, 2 mM (*C*) and 98 mM (*D*), were obtained using the same voltage clamp protocol described in *A* and *B*, respectively. Depolarization pulses during simulations were applied at the end of a 20 ms holding potential at which time test depolarizations were initiated and designated as occurring at $t = 0$ ms. A 20 ms holding potential was used to allow the channel to reach equilibrium. Data shown in *A* and *B* in this figure were obtained using the cut-open oocyte voltage clamp technique.

© The Physiological Society 2004

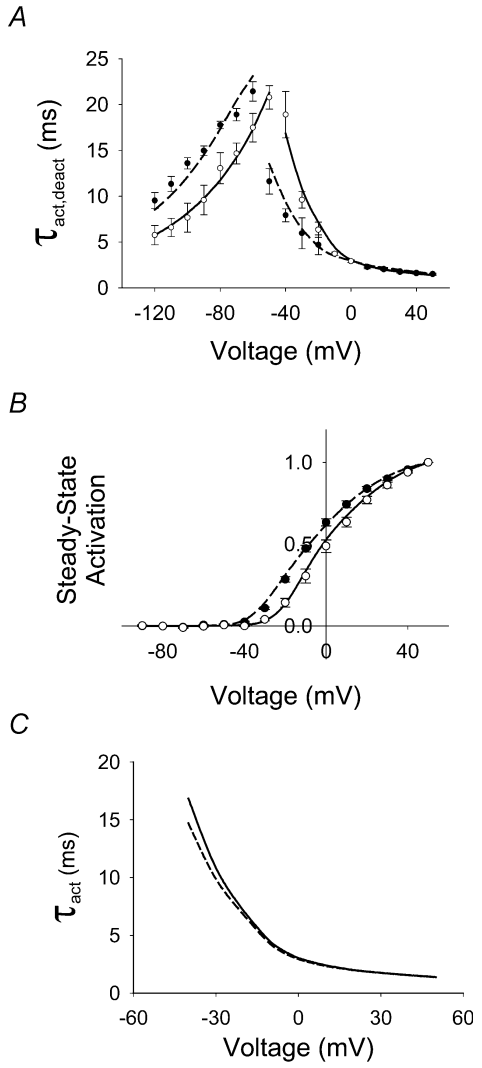

Figure 5. Comparison between simulated and experimental data

A, experimental and simulated voltage dependence of the kinetics of activation (τ_{act}) and deactivation (τ_{deact}) of the $I_{Kv4.3}$. The time constants of activation are the same as shown in Fig. 3C. The time constants of deactivation were obtained from the experimental traces of $I_{Kv4.3}$ using single exponential fitting function for 2 (○, $n = 3$) and 98 mM (●, $n = 3$) $[K^+]_o$. Unfilled and filled symbols with error bars represent plotted experimental data for 2 and 98 mM $[K^+]_o$, respectively. Continuous and dashed lines show calculated values for 2 and 98 mM $[K^+]_o$, respectively. The deactivation two-pulse protocol was the same as in Fig. 4. *B*, experimental (circles) and simulated (continuous and dashed lines) steady-state activation functions. Symbols are the same as in *A*. *C*, voltage dependence of τ_{act} obtained from simulations using the discrete state Markov model of Kv4.3 channel activation, without (continuous line) and with (dashed line) an incorporated inactivated state. Simulated data almost coincide in the voltage range from 0 to +50 mV. Small differences in the estimation of (τ_{act}) in the voltage range from −40 to 0 mV were observed. Voltage clamp protocol used for simulation is the same as in Fig. 1. Data shown in *A* and *B* in this figure were obtained using the cut-open oocyte voltage clamp technique.

potential. In high external $[K^+]$, only inward tail currents were observed.

Comparison of experimental and simulated values of time constants for activation and deactivation are plotted in Fig. 5*A* and demonstrated the close fit between the experimental and simulated values. Simulated voltage dependence for the activation time constants fitted with biexponential functions yielded equivalent charges of $0.24e_0$ and $1.39e_0$ per subunit for 2 mM $[K^+]_o$ and $0.16e_0$ and $1.21e_0$ per subunit for 98 mM $[K^+]_o$, respectively. Simulated voltage dependence of the deactivation time constants were well fitted by a single exponential function, with equivalent charges $0.48e_0$ per subunit for 2 mM $[K^+]_o$ and $0.42e_0$ per subunit for 98 mM $[K^+]_o$, respectively. Figure 5*B* shows a comparison of experimental and simulated steady-state activation relationships. Simulated data reproduced the negative shift of $V_{½}$ for steady-state activation as $[K^+]_o$ was increased from 2 to 98 mM.

A classical Hodgkin–Huxley model of activation should show a smooth bell-shaped voltage-dependent transition between τ_{act} and τ_{deact}. As shown in Fig. 5*A*, there is a steep transition between the τ_{act} and the τ_{deact} over a narrow voltage range between −60 and −40 mV at 2 mM $[K^+]_o$, which was more marked at high $[K^+]_o$. The steep transition within this voltage range can be explained by the presence of a voltage-insensitive transition between the final closed state, C_4, and the open state, O, which has different forward and reverse rate constants. The difference between these two rate constants determines the value of effective charge in the transition region and as a result the slope of the voltage dependence of τ_{act} in this region. The enhancement of the gap in values of τ_{act} and τ_{deact} at high $[K^+]_o$ reflects the slowing of deactivation.

To evaluate the possibility that our model of activation could be biased by the failure to include inactivation, we added a fast open to inactivated state transition to our model. Experimental values of fast component of inactivation at +50 mV was $\tau_{inact,fast} = 49 \pm 4$ ms ($n = 5$). The value of 50 ms used for the fast time constant of inactivation in our model closely approximates the experimental value. An inactivation time constant of 50 ms closely approximates the value for the time constant of open-state inactivation reported for Kv4.3 channels (Beck *et al.* 2002; Patel *et al.* 2002*a*). We then fitted activation kinetics obtained from simulated data that did and did not contain a fast open-inactivated state using a Hodgkin–Huxley-like activation equation $C[1 - \exp(-t/\tau_{act})]^4$ (dashed and continuous lines in Fig. 5*C*, respectively). There are no differences in τ_{act} for both models at potentials positive to 0 mV, but at negative potentials a small effect on τ_{act} was observed. In the latter

© The Physiological Society 2004

Table 1. Effects of $[K^+]_o$ on steady-state activation properties and deactivation kinetics measured with the two-electrode voltage clamp technique

$[K^+]_o$ (mM)	k (mV)	$V_{½}$ (mV)	τ_{deact}(ms)
2.0 ($n = 5$)	19.7 ± 0.7	− 31.7 ± 2.1	21.7 ± 0.8
5.0 ($n = 5$)	20.7 ± 0.7	− 32.1 ± 2.2	22.1 ± 0.7
10.0 ($n = 5$)	21.7 ± 1.2	− 30.2 ± 2.4	20.5 ± 0.6
50.0 ($n = 5$)	18.2 ± 0.7*	− 34.7 ± 1.5**	30.1 ± 2.4***

Data are expressed as means ± S.E.M. P statistics are based on comparison of data at 10 and 50 mM $[K^+]_o$. *$P < 0.03$, **$P < 0.02$, ***$P < 0.01$. τ_{deact} was measured at −45 mV.

Table 2. Model parameters

Parameter	Normal $[K^+]_o$ (2 mM)	Parameter	High $[K^+]_o$ (98 mM)
a_1	425 s^{-1}	a_{1K}	425 s^{-1}
$z_{\alpha 1}$	0.27	$z_{\alpha 1K}$	0.27
a_2	83.6 s^{-1}	a_{2K}	83.6 s^{-1}
$z_{\alpha 2}$	0.83	$z_{\alpha 2K}$	0.83
b_1	224.4 s^{-1}	b_{1K}	179.52 s^{-1}
$z_{\beta 1}$	−0.54	$z_{\beta 1K}$	−0.54
b_2	25.2 s^{-1}	b_{2K}	20.16 s^{-1}
$z_{\beta 2}$	−0.48	$z_{\beta 2K}$	−0.48
k_{co}	6000 s^{-1}	k_{co}	6000 s^{-1}
k_{oc}	1500 s^{-1}	k_{oc}	1200 s^{-1}

case, the deviation is within the error of measurements (compare with data in Fig. 5*A*). Hence, analysis of our experimental activation data should not be biased by the fast inactivation process.

Discussion

This paper is the first to describe a detailed quantitative analysis of the activation properties of Kv4.3 channels. We studied Kv4.3 activation with the cut-open voltage clamp technique in *Xenopus laevis* oocytes, a heterologous expression system that does not contain an endogenous KChIP ancillary subunit (Patel *et al.* 2002*a*). We demonstrated that: (1) activation is sigmoid and well described by a fourth power exponential function; (2) activation kinetics are voltage dependent, but the voltage dependence of activation is bi-exponential; (3) deactivation kinetics are voltage dependent and this voltage dependence is monoexponential; (4) both activation and deactivation kinetics are substantially dependent on extracellular $[K^+]$ outside of the physiological range; (5) the model closely simulated our experimental data; and (6) inclusion of fast open-state inactivation in our model has little effect on the simulations of activation.

In prior studies, limited data from different voltage clamp experiments were used to generate complex models for Kv4 family channels. The use of the standard two-electrode voltage clamp technique in oocytes typically results in capacitive transients that could obscure the initial part of the relatively fast activation process of Kv4.3 channels (Taglialatela *et al.* 1992) and as a result limits development of accurate models of activation. The studies on the gating of the Kv4.x subfamily have focused on inactivation kinetics, and as a result, studies on activation kinetics received much less attention in these investigations (Jerng & Covarrubias, 1997; Jerng *et al.* 1999; Bähring *et al.* 2001; Beck *et al.* 2002). For example, experiments on activation often used the time-to-peak current as a measure of activation kinetics (Beck *et al.* 2002). Furthermore, in the study carried out on Kv4.2 channels expressed in HEK cells, with a broader frequency band (Bähring *et al.* 2001), experiments were implemented in a cell line, which subsequently has been shown to express an endogenous KChIP protein (Patel *et al.* 2002*a*). Since, the ancillary subunit, KChIP, has been shown to modify inactivation and the recovery from inactivation, it would be highly desirable to measure Kv4.3 activation in a system that is free of the KChIP ancillary subunit. In this paper, we set out to analyse in detail the activation and deactivation processes in a Kv4.3 channel. For this purpose, we used the cut-open oocyte technique that has a wider frequency range and faster capacitance transients. This allowed us to perform quantitative measurements of both activation and deactivation.

Accurate measurement of activation kinetics can be obscured by rapid inactivation (Almers, 1978; Hille, 2001). To address this issue we used both 10 and 1000 ms test pulses. Comparison of the currents demonstrated close approximation for test pulses between 0 and +50 mV. However, a significant difference was observed for pulses between −40 and 0 mV. The value of τ_{act} at −30 mV was too long (9.6 ms) to be accurately measured by a 10 ms pulse. Hence, only the data obtained using 1000 ms test pulses, digitized at a high rate were used for development of the model for Kv4.3 channel activation. The measurement of activation in the presence of inactivation has been shown to be problematic in cases where inactivation is much faster than activation (Almers, 1978; Wang *et al.* 1997; Hille, 2001). However, in Kv4.3 channels the rate of activation exceeds the rate of inactivation by an order of magnitude, which minimizes this complication.

Activation kinetics have been studied in detail in *Shaker* (Kv1 subfamily) channels (Schoppa *et al.* 1992; Hoshi *et al.* 1994; Zagotta *et al.* 1994*a*,*b*; Aggarwal & MacKinnon, 1996; Seoh *et al.* 1996; Schoppa & Sigworth, 1998*a*,*b*,*c*; Smith-Maxwell *et al.* 1998*a*; Ledwell & Aldrich, 1999). Zagotta *et al.* (1994*a*) focused on the sigmoidicity of

© The Physiological Society 2004

activation. Using discrete state Markov models, they found that activation models of the *Shaker* K^+ channel needed at least five or six closed states and an open state to account for their activation data. In addition, the estimations of voltage dependence of *Shaker* K^+ channel open probability give an optimal fit with a fourth power of Boltzmann distribution function (Zagotta *et al.* 1994*a*). They also reported that the time constants of activation and deactivation are voltage dependent and this dependence can be described by mono-exponential functions with equivalent charges $0.42e_0$ and $1.1e_0$ per subunit, respectively. The complex Markov model developed to account for *Shaker* K^+ channel activation contained eight independent conformational changes (Zagotta *et al.* 1994*b*). In a subsequent study, Schoppa & Sigworth (1998*c*) proposed an even more complex model for activation of *Shaker* K^+ channel, containing more closed states.

Our model for activation of the Kv4.3 channel contains only five closed states, with four voltage-dependent and one voltage-independent transitions. We investigated the time course of activation development and found that the best fit is achieved with the exponential function $C[1-\exp(-t/\tau_{act})]^n$, where $n=4$ or $n=5$, but the differences between the fits were minor. Therefore, we used a model with four voltage-dependent steps to analyse Kv4.3 channel activation. In addition, we found a biexponential voltage dependence for activation time constants (Fig. 3*C*), which would appear to be at variance with prior studies on *Shaker* K^+ channels. Despite the numerous studies describing a monoexponential dependence of τ_{act} on voltage in many *Shaker* K^+ channel modelling studies, further experimentation indicated a more complex voltage dependence of τ_{act}, with larger effective charge at voltages near the activation threshold (Zagotta *et al.* 1994*a*; Schoppa & Sigworth, 1998*a*,*c*). Experimental data on Kv2.1 channel activation also indicates a more complex voltage dependence of τ_{act} (Islas & Sigworth, 1999). Deactivation kinetics of the Kv4.3 channel used in our study were monoexponential and similar to the experimental data for *Shaker* K^+ channels (Zagotta *et al.* 1994*b*) and Kv2.1 channels (Islas & Sigworth, 1999). However, other experiments with Kv4.x channels report both monoexponential (Bähring *et al.* 2001) and biexponential (Beck *et al.* 2002) time course of deactivation.

A single voltage-dependent activation step is usually characterized by an exponential dependence of the rate, or time constant. The measured time constants of activation of Kv4.3 channels in this study are complex. At very positive and very negative potentials, there is evidence of saturation of rate, indicating that a voltage-insensitive step becomes rate limiting. Our model accounts for this behaviour by a voltage insensitive final opening transition similar to that reported for other channels (Zagotta *et al.* 1994*b*; Bähring *et al.* 2001). However, taking this behaviour into account, the measured and modelled behaviour of activation and deactivation in the transition range of potentials can still not be accounted for by αs and βs with a simple exponential dependence on voltage. We chose to reconcile the fourth order sigmoid onset of the current with this complex voltage dependence with an analysis that assumes that four independent gates modulate channel activation, but that each gate has at least two populations of charge movement that operate the gate. Such an analysis yields the bi-exponential voltage dependence of τ_{act}, and we can calculate that the two charge movements yield an effective charge of $0.27e_0$ and $2.11e_0$ per subunit in 2 mM $[K^+]_o$. At extremes of potential, the larger charge movement transition is essentially instantaneous and the smaller charge movement governs activation and deactivation voltage dependence. However, at intermediate potentials (i.e. near threshold of activation) the larger charge component dominates, giving rise to the steep voltage dependence of the time constants of activation and deactivation in this range.

The slope of the steady-state activation relationship, which has been used to estimate the effective gating charge, was 19.4 mV at 2 mM $[K^+]_o$, which corresponds to values reported by Smith-Maxwell *et al.* (1998*a*), Bähring *et al.* (2001) and Beck *et al.* (2002). The voltage dependence of steady-state open probability was obtained from experiments in which the limiting slope approach was used to minimize the error introduced by inactivation (Almers, 1978). The steepness of the voltage dependence of gating current measurements provided estimates of gating charge movement that were approximately double the values obtained from the data showing the voltage dependence of the relative conductance of the channel (Hille, 2001). The steady-state activation relation in Kv4.3 channels is ~2–3 times less steep than it is for *Shaker* K^+ channels (Smith-Maxwell *et al.* 1998*a*; Hille, 2001; Beck *et al.* 2002). A comparison of the amino acid sequence between the S4 of Kv4.3 and *Shaker* K^+ channels reveals significant differences (Fig. 6). First, the S4 region of Kv4.3 channels contains two fewer positive charges than in *Shaker* K^+ channels. Although the outer four charges make the largest contribution to gating charge, the neutralization of the first charged residue in Kv4.3 channels cannot fully account for the difference in slope factor between Kv4.3 and *Shaker* K^+ channels (Aggarwal & MacKinnon, 1996). Comparison of these S4 regions also shows seven differences among the uncharged residues, six of which

© The Physiological Society 2004

are in the outer portion of S4 (Fig. 6). These uncharged residues may be important because Lopez *et al.* (1991), McCormack *et al.* (1991) and Smith-Maxwell *et al.* (1998*b*) have shown that they can also affect the kinetic, steady-state and voltage-dependent properties of K^+ channels. Finally, the impact of the recent structural studies on S4 suggests a more complex model of S4 position and movement during activation than previously suspected (Gonzalez *et al.* 2000; Jiang *et al.* 2003*b*; Cohen *et al.* 2003). Perhaps the relatively shallow, complex voltage dependence of τ_{act}, reflects a more complex movement of S4 charge than that described by the sliding helix model (Catterall, 1986).

Effects of extracellular K^+ concentration

Our experimental data show no substantial dependence of activation and deactivation on the extracellular $[K^+]$ in the range from 2 to 10 mM. However, we found that an increase in $[K^+]_o$ from 10 to 98 mM had significant effects on channel gating. With the cut-open oocyte data, we found that the increase in $[K^+]_o$ from 2 to 98 mM slows deactivation and speeds activation by shifting its voltage dependence to negative values. Similar effects of elevated $[K^+]_o$ on deactivation were observed in the delayed rectifier K^+ currents in squid axon and on activation in Kv4.3 channels (Swenson & Armstrong, 1981; Eghbali *et al.* 2002; Shahidullah & Covarrubias, 2003). These findings are in contrast to those for *Shaker* K^+ (Zagotta *et al.* 1994*b*) and HERG channels (Wang *et al.* 1997), where $[K^+]_o$ had no effect on activation and deactivation. In addition to the effects of high extracellular $[K^+]$ on the delayed rectifier K^+ currents, Swenson & Armstrong (1981) reported that in the squid giant axon, Rb^+ slowed deactivation of this K^+ current. Rb^+ had similar effects on Kv4.2 deactivation (Bähring *et al.* 2001; Shahidullah & Covarrubias, 2003). Thus, our data along with the data of others mentioned above support the view that increased occupancy of an outer cation binding site, whether due to increased concentration or increased affinity for the channel binding site, inhibits the channel from making its transition from the open state to a non-conducting closed state. The appearance of an effect on deactivation kinetics only at high $[K^+]_o$ suggests that the dissocation kinetics of K^+ from its binding site are too rapid for an effect to be seen at physiological $[K^+]_o$.

In our experiments, the effect of increased $[K^+]_o$ on the rate of deactivation is likely to be associated with increased occupancy of the outer binding site in the channel pore. Hence, we suggest that the presence of K^+ in the outer pore region of the Kv4.3 channel stabilizes the open state and slows deactivation. These data suggest that the gate responsible for deactivation is different in Kv4.x from that in *Shaker* and HERG. In *Shaker* K^+ channels, an activation gate has been localized to the intracellular face of the pore, particularly on S6 (Jan & Jan, 1994; del Camino & Yellen, 2001; Perozo, 2002), although additional 'gates' have been suggested. One interpretation of our K^+ dependence data is that occupancy of the pore modulates activation through an allosteric linkage between pore occupancy and an intracellular gate as has been proposed based on the crystal structure of KcsA (Doyle *et al.* 1998). A simpler interpretation is that Kv4.3 activation is controlled by an extracellular gate. This hypothesis is supported by the drug binding evidence in native and cloned Kv4.x channels that the intracellular pore mouth remains open at rest (Campbell *et al.* 1993; Tseng *et al.* 1996; Yeola & Snyders, 1997). While our data do not allow us to distinguish between allosteric modulation of an intracellular gate and direct gating at the extracellular pore, there is clear evidence from this study and the work of others, for the involvement of permeant ions in stabilizing the open conformation of the channel (Eghbali *et al.* 2002).

Figure 6. Comparison of the S4 sequences in *Shaker* and Kv4.3
The S4 in Kv4.3 has two fewer charges than in *Shaker*. In addition, there are seven other differences in the uncharged residues.

References

Aggarwal SK & MacKinnon R (1996). Contribution of the S4 segment to gating charge in the *Shaker* K^+ channel. *Neuron* **16**, 1169–1177.

Almers W (1978). Gating currents and charge movements in excitable membranes. *Rev Physiol Biochem Pharmacol* **82**, 96–190.

An WF, Bowlby MR, Betty M, Cao J, Ling HP, Mendoza G, Hinson JW, Mattsson KI, Strassle BW, Trimmer JS & Rhodes KJ (2000). Modulation of A-type potassium channels by a family of calcium sensors. *Nature* **403**, 553–556.

Antzelevitch C & Shimizu W (2002). Cellular mechanisms underlying the long QT syndrome. *Curr Opin Cardiol* **17**, 43–51.

Bähring R, Boland LM, Varghese A, Gebauer M & Pongs O (2001). Kinetic analysis of open- and closed-state inactivation transitions in human Kv4.2 A-type potassium channels. *J Physiol* **535**, 65–81.

Beck EJ, Bowlby M, An WF, Rhodes KJ & Covarrubias M (2002). Remodelling inactivation gating of Kv4 channels by KChIP1, a small-molecular-weight calcium-binding protein. *J Physiol* **538**, 691–706.

© The Physiological Society 2004

Beck EJ & Covarrubias M (2001). Kv4 channels exhibit modulation of closed-state inactivation in inside-out patches. *Biophys J* **81**, 867–883.

Bezanilla F & Armstrong CM (1977). Inactivation of the sodium channel. I. Sodium current experiments. *J General Physiol* **70**, 549–566.

Brahmajothi MV, Campbell DL, Rasmusson RL, Morales MJ, Trimmer JS, Nerbonne JM & Strauss HC (1999). Distinct transient outward potassium current (I_{to}) phenotypes and distribution of fast-inactivating potassium channel alpha subunits in ferret left ventricular myocytes. *J General Physiol* **113**, 581–600.

Campbell DL, Qu Y, Rasmusson RL & Strauss HC (1993). The calcium-independent transient outward potassium current in isolated ferret right ventricular myocytes. II. Closed state reverse use-dependent block by 4-aminopyridine. *J General Physiol* **101**, 603–626.

Campbell DL, Rasmusson RL, Comer MB & Strauss HC (1995). The cardiac calcium-independent transient outward potassium current: kinetics, molecular properties, and role in ventricular repolarization. In *Cardiac Electrophysiology. From Cell to Bedside*, 2nd edn, ed.Zipes D & Jalife J, pp. 83–96. W.B. Saunders Co, Philadelphia.

Catterall WA (1986). Voltage-dependent gating of sodium channels: Correlating structure and function. *Trends Neurosci* **9**, 7–10.

Cohen BE, Grabe M & Jan LY (2003). Answers and questions from the KvAP structures. *Neuron* **39**, 395–400.

Comer MB, Campbell DL, Rasmusson RL, Lamson DR, Morales MJ, Zhang Y & Strauss HC (1994). Cloning and characterization of an I_{to}-like potassium channel from ferret ventricle. *Am J Physiol* **267**, H1383–H1395.

del Camino D & Yellen G (2001). Tight steric closure at the intracellular activation gate of a voltage-gated K^+ channel. *Neuron* **32**, 649–656.

Doyle DA, Morais Cabral J, Pfuetzner RA, Kuo A, Gulbis JM, Cohen SL, Chait BT & MacKinnon R (1998). The structure of the potassium channel: Molecular basis of K^+ conduction and selectivity. *Science* **280**, 69–77.

Eghbali M, Olcese R, Zarei MM, Toro L & Stefani E (2002). External pore collapse as an inactivation mechanism for Kv4.3 K^+ channels. *J Memb Biol* **188**, 73–86.

Gebauer M, Isbrandt D, Sauter K, Callsen B, Nolting A, Pongs O & Bähring R (2004). N-type inactivation features of Kv4.2 channel gating. *Biophys J* **86**, 210–223.

Gonzalez C, Rosenman E, Bezanilla F, Alvarez O & Latorre R (2000). Modulation of *Shaker* K^+ channel gating kinetics by the S3–S4 linker. *J Gen Physiol* **115**, 193–207.

Hille B (2001). *Ion Channels of Excitable Membranes*, 3rd edn. Sinauer Associates, Sunderland, MA, USA.

Hoshi T, Zagotta WN & Aldrich RW (1991). Two types of inactivation in *Shaker* K^+ channels: effects of alterations in the carboxy-terminal region. *Neuron* **7**, 547–556.

Hoshi T, Zagotta WN & Aldrich RW (1994). *Shaker* potassium channel gating I: Transitions near the open state. *J General Physiol* **103**, 249–278.

Islas LD & Sigworth FJ (1999). Voltage sensitivity and gating charge in *Shaker* and *Shab* family potassium channels. *J Gen Physiol* **114**, 723–742.

Jan LY & Jan YN (1994). Potassium channels and their evolving gates. *Nature* **371**, 119–122.

Jerng HH & Covarrubias M (1997). K^+ channel inactivation mediated by the concerted action of the cytoplasmic N- and C-terminal domains. *Biophys J* **72**, 163–174.

Jerng HH, Shahidullah M & Covarurubias M (1999). Inactivation gating of Kv4 potassium channels. Molecular interactions involving the inner vestibule of the pore. *J General Physiol* **113**, 641–659.

Jiang X, Bett GC, Li X, Bondarenko VE & Rasmusson RL (2003*a*). C-type inactivation involves a significant decrease in the intracellular aqueous pore volume of Kv1.4 K^+ channels expressed in *Xenopus* oocytes. *J Physiol* **549**, 683–695.

Jiang Y, Ruta V, Chen J, Lee A & MacKinnon R (2003*b*). The principle of gating charge movement in a voltage-dependent K^+ channel. *Nature* **423**, 42–48.

Ledwell JL & Aldrich RW (1999). Mutations in the S4 region isolate the final voltage-dependent cooperative step in potassium channel activation. *J General Physiol* **113**, 389–414.

Liu Y, Jurman ME & Yellen G (1996). Dynamic rearrangement of the outer mouth of a K^+ channel during gating. *Neuron* **16**, 859–867.

Lopez GA, Jan YN & Jan LY (1991). Hydrophobic substitution mutations in the S4 sequence alter voltage-dependent gating in *Shaker* K^+ channels. *Neuron* **7**, 327–336.

McCormack K, Tanouye MA, Iverson LE, Lin JW, Ramaswami M, McCormack T, Campanelli JT, Mathew MK & Rudy B (1991). A role for hydrophobic residues in the voltage-dependent gating of *Shaker* K^+ channels. *Proc Natl Acad Sci USA* **88**, 2931–2935.

Näbauer M, Beuckelmann DJ & Erdmann E (1993). Characteristics of transient outward current in human ventricular myocytes from patients with terminal heart failure. *Circ Res* **73**, 386–394.

Nerbonne JM (2000). Molecular basis of functional voltage-gated K^+ channel diversity in the mammalian myocardium. *J Physiol* **525**, 285–298.

Nerbonne JM, Nichols CG, Schwarz TL & Escande D (2001). Genetic manipulation of cardiac K^+ channel function in mice. What have we learned, and where do we go from here? *Circ Res* **89**, 944–956.

Papazian DM, Timple LC, Jan YN & Jan LY (1991). Alteration of voltage-dependence of *Shaker* potassium channel by mutations in the S4 sequence. *Nature* **349**, 305–310.

Patel SP, Campbell DL, Morales MJ & Strauss HC (2002*a*). Heterogeneous expression of KChIP2 isoforms in the ferret heart. *J Physiol* **539**, 649–656.

© The Physiological Society 2004

Patel SP, Campbell DL & Strauss HC (2002*b*). Elucidating KChIP effects on Kv4.3 inactivation and recovery kinetics with a minimal KChIP2 isoform. *J Physiol* **545**, 5–11.

Perozo E (2002). New structural perspectives on K^+ channel gating. *Structure* **10**, 1027–1029.

Rasmusson RL, Morales MJ, Castellino RC, Zhang Y, Campbell DL & Strauss HC (1995). C-type inactivation controls recovery in a fast inactivating cardiac K^+ channel (Kv1.4) expressed in *Xenopus* oocytes. *J Physiol* **489**, 709–721.

Rasmusson RL, Morales MJ, Wang S, Liu S, Campbell DL, Brahmajothi MV & Strauss HC (1998). Inactivation of voltage-gated cardiac K^+ channels. *Circ Res* **82**, 739–750.

Rosati B, Grau F, Rodriguez S, Li H, Nerbonne JM & McKinnon D (2003). Concordant expression of KChIP2 mRNA, protein and transient outward current throughout the canine ventricle. *J Physiol* **548**, 815–822.

Schoppa NE, McCormack K, Tanouye MA & Sigworth FJ (1992). The size of gating charge in wild-type and mutant *Shaker* potassium channels. *Science* **255**, 1712–1715.

Schoppa NE & Sigworth FJ (1998*a*). Activation of *Shaker* potassium channels. I. Characterization of voltage-dependent transitions. *J General Physiol* **111**, 271–294.

Schoppa NE & Sigworth FJ (1998*b*). Activation of *Shaker* potassium channels. II. Kinetics of the V2 mutant channel. *J General Physiol* **111**, 295–311.

Schoppa NE & Sigworth FJ (1998*c*). Activation of *Shaker* potassium channels. III. An activation gating model for wild-type and V2 mutant channels. *J General Physiol* **111**, 313–342.

Seoh SA, Sigg D, Papazian DM & Bezanilla F (1996). Voltage-sensing residues in the S2 and S4 segments of the *Shaker* K^+ channel. *Neuron* **16**, 1159–1167.

Shahidullah M & Covarrubias M (2003). The link between ion permeation and inactivation gating of Kv4 potassium channels. *Biophys J* **84**, 928–941.

Smith-Maxwell CJ, Ledwell JL & Aldrich RW (1998*a*). Role of the S4 in cooperativity of voltage-dependent potassium channel activation. *J General Physiol* **111**, 399–420.

Smith-Maxwell CJ, Ledwell JL & Aldrich RW (1998*b*). Uncharged S4 residues and cooperativity in voltage-dependent potassium channel activation. *J General Physiol* **111**, 421–439.

Strauss HC, Morales MJ, Wang S, Brahmajothi MV & Campbell DL (2001). Voltage dependent K^+ channels. In *Heart Physiology and Pathophysiology*, 4th edn, ed.Sperelakis N, Kurachi Y, Terzic A & Cohen MV, pp. 259–280. Academic Press, San Diego, CA, USA.

Swenson RP & Armstrong CM (1981). K^+ channels close more slowly in the presence of external K^+ and Rb^+. *Nature* **291**, 427–429.

Taglialatela M, Toro L & Stefani E (1992). Novel voltage clamp to record small, fast currents from ion channels expressed in *Xenopus* oocytes. *Biophys J* **61**, 78–82.

Tseng GN, Jiang M & Yao JA (1996). Reverse use dependence of Kv4.2 blockade by 4-aminopyridine. *J Pharmacol Exp Ther* **279**, 865–876.

Wang S, Liu S, Morales MJ, Strauss HC & Rasmusson RL (1997). A quantitative analysis of the activation and inactivation kinetics of HERG expressed in *Xenopus* oocytes. *J Physiol* **502**, 45–60.

Wang S, Patel SP, Qu Y, Hua P, Strauss HC & Morales MJ (2002). Kinetic properties of Kv4.3 and their modulation by KChIP2b. *Biochem Biophys Res Commun* **295**, 223–229.

Yeola SW & Snyders DJ (1997). Electrophysiological and pharmacological correspondence between Kv4.2 current and rat cardiac transient outward current. *Cardiovasc Res* **33**, 540–547.

Zagotta WN, Hoshi T, Dittman J & Aldrich RW (1994*a*). *Shaker* potassium channel gating II: Transitions in the activation pathway. *J General Physiol* **103**, 279–319.

Zagotta WN, Hoshi T & Aldrich RW (1994*b*). *Shaker* potassium channel gating III. Evaluation of kinetic models for activation. *J General Physiol* **103**, 321–362.

Acknowledgements

This work was supported in part by National Heart, Lung, and Blood Institute grants 19216, 52874 and 62465, the NSF KDI – DBI-9873173, a grant from the American Heart Association and a grant from the Oishei Foundation.

© The Physiological Society 2004